Performance Evaluation of a Zerovalent Iron Reactive Barrier: Mineralogical Characteristics

ARTICLE *in* ENVIRONMENTAL SCIENCE AND TECHNOLOGY · OCTOBER 2000

Impact Factor: 5.33 · DOI: 10.1021/es001005z

Environ. Sci. Technol. **2000**, *34,* 4169−4176

Performance Evaluation of a Zerovalent Iron Reactive Barrier: Mineralogical Characteristics

D. H. PHILLIPS,* B. GU, D. B. WATSON, Y. ROH, L. LIANG, AND S. Y. LEE

Environmental Sciences Division, Oak Ridge National Laboratory, P.O. Box 2008, Building 1505, Oak Ridge, Tennessee 37831

There is a limited amount of information about the effects of mineral precipitates and corrosion on the lifespan and long-term performance of in situ Fe^0 reactive barriers. The objectives of this paper are (1) to investigate mineral precipitates through an in situ permeable Fe^0 reactive barrier and (2) to examine the cementation and corrosion of Fe^0 filings in order to estimate the lifespan of this barrier. This field scale barrier (225′ long × 2′ wide × 31′ deep) has been installed in order to remove uranium from contaminated groundwater at the Y-12 plant site, Oak Ridge, TN. According to XRD and SEM-EDX analysis of core samples recovered from the Fe^0 portion of the barrier, iron oxyhydroxides were found throughout, while aragonite, siderite, and FeS occurred predominantly in the shallow portion. Additionally, aragonite and FeS were present in up-gradient deeper zone where groundwater first enters the Fe^0 section of the barrier. After 15 months in the barrier, most of the Fe^0 filings in the core samples were loose, and a little corrosion of Fe^0 filings was observed in most of the barrier. However, larger amounts of corrosion (∼10−150 μm thick corrosion rinds) occurred on cemented iron particles where groundwater first enters the barrier. Bicarbonate/carbonate concentrations were high in this section of the barrier. Byproducts of this corrosion, iron oxyhydroxides, were the primary binding material in the cementation. Also, aragonite acted as a binding material to a lesser extent, while amorphous FeS occurred as coatings and infilings. Thin corrosion rinds (2−50 μm thick) were also found on the uncemented individual Fe^0 filings in the same area of the cementation. If corrosion continues, the estimated lifespan of Fe^0 filings in the more corroded sections is 5 to 10 years, while the Fe^0 filings in the rest of the barrier perhaps would last longer than 15 years. The mineral precipitates on the Fe^0 filing surfaces may hinder this corrosion but they may also decrease reactive surfaces. This research shows that precipitation will vary across a single reactive barrier and that greater corrosion and subsequent cementation of the filings may occur where groundwater first enters the Fe^0 section of the barrier.

Introduction

Recently, Fe^0 permeable reactive barrier technology has received much interest as an alternative to pump and treat systems because Fe^0 is a readily available medium that is cost saving over a long term and has shown encouraging results in remediating contaminants from groundwater (*1*−*20, 24, 26, 27, 30*−*32*). Most of the Fe^0 systems are used to mediate volatile organic compounds by reductive dehalogenation (*1, 2*), and only a few are used to remove heavy metals (*3, 4*) and radionuclides (*5*−*8*). Over 12 of each full- and pilot-scale in situ Fe^0 permeable reactive barriers have been installed in North America (*9*). However, only a few studies (*6, 10*−*12*) have addressed issues related to the long-term performance of Fe^0 as a reactive barrier material. Currently, there is still much uncertainty in predicting long-term effectiveness of the reactive media and the hydraulic performance of these permeable barriers at long-run time (*10*).

Geochemical conditions within in situ Fe^0 permeable reactive barriers are responsible for the corrosion of Fe^0 filings (*2*) and the formation of precipitates (*10*). Mineral precipitates in Fe^0 reactive barriers may decrease surface reactivity, thus influencing the effectiveness and lifespan of the barrier (*6, 10*−*12*). Because the geochemistry of the groundwater varies at different barrier sites, the types and extent of mineral precipitation vary broadly at different barriers. For example, green rust, $[Fe_4^{2+}Fe_3^{2+}(OH)_{12}][SO_4^{2-}\cdot 2H_2O]$, was observed in the Fe^0 barrier at the Elizabeth City, NC and Lowry Air Force Base, CO site (installed in 1995) where SO_4^{2-} was partially reduced in the groundwater (*13*). Calcium and Fe carbonate precipitated in a gate in the Fe^0 medium of the permeable reactive barrier at the Denver Federal Center, Denver, CO where carbonate was high in the groundwater (*14*). Conversely, a reactive barrier in Borden, ON showed no mineral precipitation after one year of operation, even though losses of 185 mL/L Ca^{2+} and 82 mL/L of HCO_3^- were detected across the barrier (*11*).

Depletion of reactive media through corrosion is also a concern in long-term performance of Fe^0 barriers (*11*). Agents corrosive to Fe^0, such as HCO_3^- and SO_4^{2-} (*15*), commonly occur in groundwater (*6*) and are expected to cause Fe^0 filings to disintegrate in reactive barriers. Measurements of disintegration rates of Fe^0 filings in their perspective geochemical environments are needed to predict future excavation or renewal of the barrier material. The accumulation of some precipitates, either individually or as a mixture, such as iron and calcium carbonate (*11, 16*), green rust (*17*), and iron oxyhydroxides (*12*), may restrict flow and eventually clog the system (*10, 11*).

Application of Fe^0 technology for the remediation of uranium from groundwater is being investigated at the Oak Ridge National Laboratory (*5, 6*). A pilot-scale in situ Fe^0 permeable reactive barrier was installed in late November 1997 at the Bear Creek Valley (BCV) Y-12 Plant, Oak Ridge, TN, to intercept uranium contaminated groundwater (*18*). A long-term monitoring plan of the groundwater and barrier material at the site is being carried out. The objectives of this paper are to report (1) the minerals that have precipitated along the barrier and (2) to examine the cementation and corrosion of Fe^0 filings that have occurred over the first 15 months of operation in order to estimate the lifespan of the barrier.

Materials and Methods

Barrier Installation. In late November of 1997, GeoCon Inc. completed construction of the Fe^0 barrier at the Oak Ridge Y-12 site (Figure 1a). The barrier dimension is ∼225′ long × 2′ wide with an Fe^0 filled midsection of ∼31′ deep × 26′ long) between two 99.5′ sections of pea gravel. The pea gravel

* Corresponding author phone: (865)241-3959; fax: (865)576-3989; e-mail: phillipsdh@ornl.gov.

10.1021/es001005z
Published on Web 08/31/2000

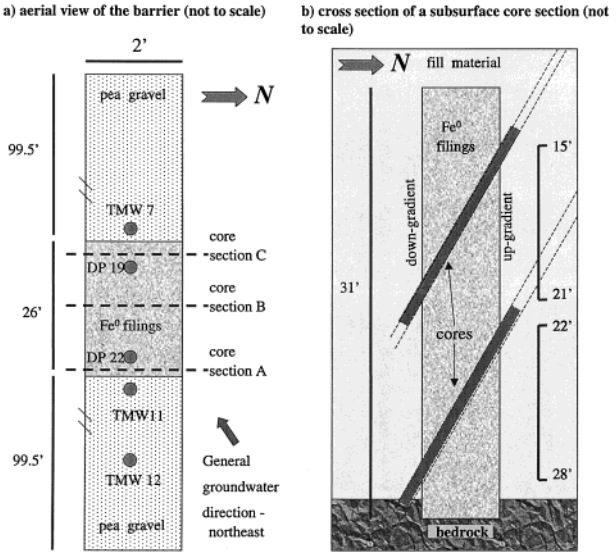

FIGURE 1. Diagrams of the barrier at the Bear Creek Valley Y-12 plant site, Oak Ridge, TN (not to scale): (a) aerial view of the barrier showing the groundwater flow direction and sampling locations for groundwater and cores and (b) subsurface cross section of a coring section.

sections are used to increase groundwater flow through the Fe^0 treatment media and divert it down-gradient. Guar gum biopolymer slurry was used to prevent sloughing during soil excavation (*19*). The Fe^0 filings used in the reactive barrier were obtained from Peerless Metal Powders and Abrasives, Detroit, MI. These Fe^0 filings are ~3 to 24 mm long (majority at ≥10 mm) and 0.5 to 1.5 mm thick (about −1/2 and 25 mesh size). These Fe^0 filings were composed of about 86% Fe^0, 3−4% carbon, 3% silicon and other elements, and small amounts of magnetite (Fe_3O_4) (*20*). The material around the barrier is a heterogeneous mixture of fill materials and native soil, saprolite, and rock fragments. Native soil and saprolite from the Nolichucky Shale formation are present near the bottom of the barrier (*18*).

Groundwater Characteristics. The background well (TMW 12) is situated in the up-gradient section of the pea gravel in the barrier where much of the untreated groundwater collects before moving down through the Fe^0 portion of the barrier (Figure 1a). The groundwater from the background well is mainly aerobic with a near neutral pH and generally higher concentrations of HCO_3^-/CO_3^-, Ca^{2+}, SO_4^{2-}, NO_3^- compared to the groundwater in the barrier (Table 1; Figure 2). Similar Fe^{2+} and S^- values are observed for the groundwater from TMW 12 and piezometers from the Fe^0 section of the trench. The background uranium concentration of this groundwater in the up-gradient soil and pea gravel portion of the barrier is generally <2 mg/L. The pea gravel portion of the trench had uranium concentrations of 0.02 to 0.7 mg/L. Uranium in the groundwater generally decreases greatly within the barrier (*18*). However, uranium minerals were not detected in these core samples which maybe due to a combination of the following factors: (1) the precipitation of such a small amount of U minerals that they were below detection limits, (2) the low concentration of uranium in the groundwater, and (3) the short length of time in which the barrier has been in operation. The decrease in U in the groundwater within the barrier material is probably due to reductive precipitation of uranium which formed insoluble U(IV) species onto the surface of the Fe^0 filings and corrosion byproducts (*5*).

Hydrology. Bromide tracer tests indicate that groundwater generally flows toward the barrier from the northeast direction; however, it may also enter the Fe^0 treatment zone of the barrier from northern and eastern up-gradient flow directions (*18*) (Figure 1a). Once in the Fe^0 barrier, the groundwater migrates preferentially through the porous filings and exits at the southern and western down-gradient ends. There does not appear to be any significant seasonal differences in the general groundwater flow patterns between spring and fall when groundwater levels are at their highest and lowest, respectively. The overall horizontal gradient across the site is 0.025 in May; however, the gradient in the immediate vicinity of the trench is only 0.01. The overall gradient in October was 0.02 and 0.009 in close proximity to the barrier. A flattening of the hydraulic gradient near the barrier is expected due to the high hydraulic conductivity of the gravel and iron filings backfill. Based on a bromide tracer test, an average interstitial groundwater flow rate of approximately 2.2 m/day is estimated, or approximately 11.9 L/min is flowing through the iron barrier by assuming an effective porosity of 0.2 (*18*). However, seasonal changes in groundwater levels are as much as 2 to 3′ with groundwater levels being the highest in the winter and spring and lowest in the late fall. Groundwater levels in wells can increase rapidly (1′ within hours) during storm events with recession curves lasting several days. Upward hydraulic gradients, as high as 0.12′/feet, were also observed between a bedrock well (34′ deep) and shallow well (17′ deep) screened in the unconsolidated zone, as evidenced by the presence of relatively high nitrate concentrations in the deep ports of several multilevel sampling wells (*18*).

Groundwater Analysis. A total of 47 piezometers or monitoring wells were installed around the trench (*18*) in addition to other sampling ports near the study area. However, this report focuses on groundwater samples from an up-gradient background well (TMW 12) (40′ to the north) in the gravel and 2 multilevel piezometers (DP 19, DP 22) inside the Fe^0 filing portion of the barrier near where the cores were sampled (Figure 3). Filtered groundwater samples at DP 19 and DP 22 were each collected at vertical depths of 18′ and 26′ every 2 months over an 18-month period for chemical analysis (*18*). Samples were both acidified (pH<2) and nonacidified. From the acidified samples, Ca was analyzed using a Thermo Jarrell Ash inductively coupled plasma PolyScan Iris Spectrometer. Additionally, groundwater pH and Eh were collected as field parameters with a Yellow Springs Instruments XL600M multiparameter probe. Bicarbonate/carbonate was determined by analysis of total inorganic carbon with a Shimadzu total organic carbon analyzer (TOC−5000A, Tokyo, Japan) in unacidified water samples. Total U in the acidified water samples was analyzed using a kenetic phosphorescence lifetime analyzer (Chem-Chek, KPA−11). Sulfate and NO_3^- in the unacidified water samples was measured by ion chromatography (Dionex 500, Sunnyvale CA). In the field, Fe^{2+} was determined using the 1, 10 phenanthroline procedure and S^- was measured with the methylene blue method (Hach DR/2000 Spectrophotometer Handbook, Loveland CA).

Analysis of Core Material. About 15 months after the barrier was installed, cores were collected in polyurethane tubes (4′ length × 1 1/4″ dia.) from the Fe^0 filing portion and adjacent fill material with a Geoprobe by Miller, Huntsville, AL. The northern up-gradient and southern down-gradient interfaces of the barrier and soil/fill material were intercepted by coring at 60-degree angles (Figure 1b). The cores were taken from three sections (A, B and C) (Figure 1a) along the Fe^0 barrier at ~14−22′ and ~21−29′ levels. This was done by driving a hollow barrel through the fill material to the area of the barrier in which the cores were to be taken. Two to three cores where taken from each sampling point by driving the corer containing the polyurethane tubes through the hollow barrel into the barrier material. The polyurethane tube was cut to size and sealed with plastic caps immediately

TABLE 1. Geochemical Parameters of the Groundwater from the Up-Gradient Background (TMW 12) Well and the Multilevel Piezometers (DP19 and DP 22) within the Fe^0 Portion of the Barrier

			mg/L						
location	pH	Eh, mV	HCO_3^-/CO_3^-	Ca^{2+}	Fe^{2+}	SO_4^{2-}	S^-	total U	NO_3^-
				Background					
TMW12	6.6−6.8	210− −110	330−650	160−220	0−4.8	63−170	0−0.05	0.02−0.7	10.3−130
				Within the Fe^0 Portion of the Trench					
				Up-Gradient					
DP22S 14′−22′	6.7−7.5	−320− −130	390−540	40−160	2−330	17−104	0−0.02	0.03−0.25	0−5.3
DP22M 21′−29′	5.9−6.9	−130− −3.5	460−590	170−190	0.08−2.14	70−150	0.001−0.04	0.22−0.57	2.42−68.3
				Down-Gradient					
DP19S 14′−22′	7.0−8.3	−240− −160	17−430	21−130	0.4−14.5	30−90	0.003−0.02	0.0007−0.02	0.02−47.4
DP19M 21′−29′	7.2−10.4	−310− −170	60−330	5−21	0−0.14	0.10−60	0−0.02	0.00002−0.04	0.1−0.24

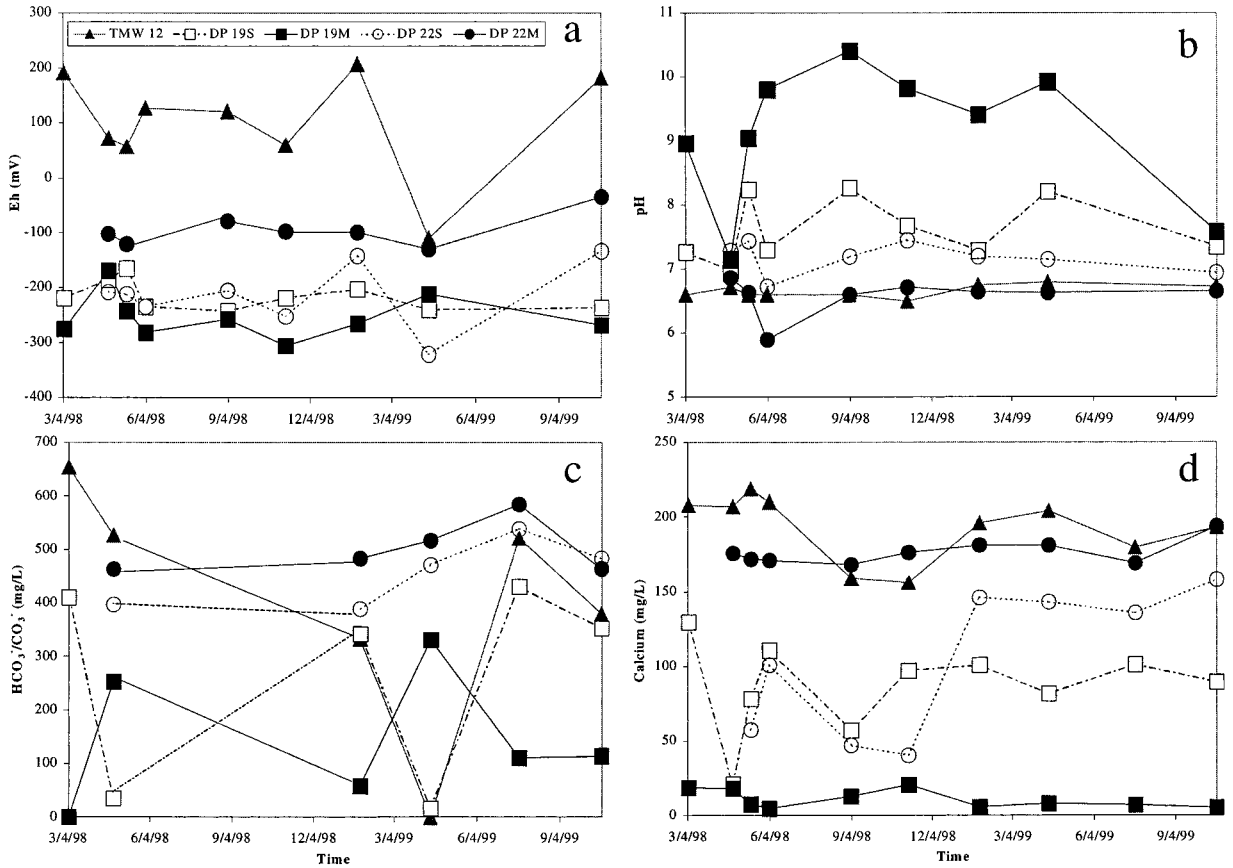

FIGURE 2. Groundwater geochemical parameters influenced the precipitation of minerals throughout the Fe^0 barrier: (a) Eh, (b) pH, (c) bicarbonate/carbonate, and (e) calcium.

after they were removed from the barrier. Argon was injected into the cores through small incisions at each end of the plastic caps. These incisions were immediately sealed with tape after injection. The cores were stored in Ar purged airtight PVC tubes to minimize oxidation. During the period betweensampling and preparation (2−3 weeks), the PVC storage tubes were purged with Ar twice a week.

Because of disturbances, mainly compaction and spillage that resulted in about 50% retrieval of the cores, generally only ∼2′ of core material were actually collected in each 4′ core tube. Therefore, two cores were collected from each sampling point in order to retrieve both up- and down-gradient interfaces of the barrier. Together, the cores from each of the sampling points usually contained about 0.5′ of soil and fill material from each interface and about 3′ of barrier material. During preparation, the barrier material from each coring point was separated into 4 segments (usually ∼5″ long). Representative samples (∼10 g) of each segment, including cemented samples, were immediately rinsed with acetone, brought to dryness, and used for mineralogical and morphological analysis.

For X-ray diffraction (XRD) analysis, the dried samples were sonicated in acetone for 2 h to detach precipitates from Fe^0 filings. To avoid destruction of the filter from the acetone, an aliquot of the mineral suspension in acetone was pipetted into Milli-Q water (acetone:H_2O = 1:1) and vacuum plated onto 0.45 μm Millipore filters. Mineralogical characterization of these mounts was performed with XRD using a Scientag

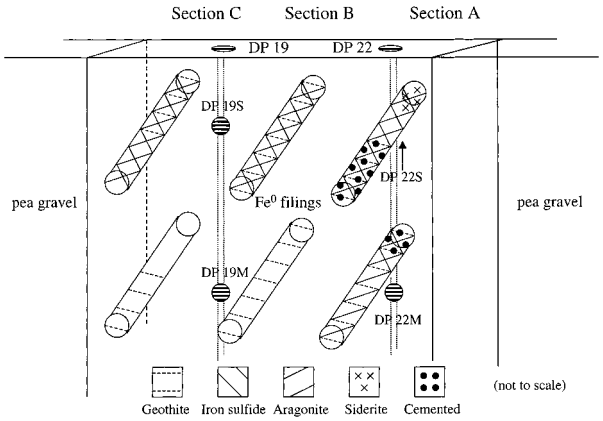

FIGURE 3. The distribution of the mineralogy of the cores from the Fe^0 portion of the barrier. Note: akaganeite which is not shown in the diagram was present throughout the cores from the barrier.

XDS−2000 diffractometer operated at 45 kV and 40 mA (Sunnyvale, CA (*21*)).

The nonsonicated acetone processed samples were vacuum-dried on a Buckner funnel. Zerovalent iron filings and corrosion byproducts were separated using tweezers, and small amounts of each were secured to Al stubs. These samples were carbon coated with a Bio-Rad carbon sputter coater and immediately examined with a JEOL ISM 35CF scanning electron microscope equipped with an energy dispersive X-ray analyzer (EDX) (Tokyo, Japan) (*21*) in order to investigate mineral morphology and determine the chemical composition of the minerals semiquantitatively by EDX analysis. Selected individual Fe^0 filings and cemented samples were impregnated with epoxy, sawed in half, and polished. These polished sections were also observed and analyzed with the SEM-EDX. Visual estimates of the lifespan of the Fe^0 filings were made based on corrosion and mineral precipitates on Fe^0 filings from these polished sections.

Results and Discussion

Mineral Precipitates and Associated Geochemical Parameters. After 15 months of burial under reduced (anaerobic) conditions, Fe^0 filings and fine corrosion byproducts appeared black and loose in most sections of the cores, except in Section A where cemented Fe^0 filings were recovered in small areas. These cemented areas were 18−21′ below the surface in the upper portion of Section A near the southern down-gradient interface of fill and barrier material (Figure 3). An additional cemented area was present in Section A at the northern up-gradient soil/fill and barrier interface at a vertical depth of 22′. Clean contact between the Fe^0 barrier and surrounding fill material, consisting of soil, rock fragments, and native bedrock, revealed little mixing of surrounding soil/fill with the barrier material; therefore, most of the mineral precipitates found in the barrier were formed in situ. Scanning electron microscopy with EDX and XRD analysis revealed a suite of minerals within the Fe^0 barrier that include goethite (α-FeOOH), akaganeite (β-FeOOH), FeS, aragonite ($CaCO_3$) and siderite ($FeCO_3$) (Figures 3 and 4a−d).

Iron Oxyhydroxide (FeOOH) Precipitates. The most widely occurring corrosion byproducts, Fe oxyhydroxides, were detected by XRD throughout the Fe^0 barrier (Figure 3). These minerals form as a result of the corrosion of Fe^0 filings in groundwater with a concurrent release of Fe^{2+} and an increased pH (*22*). The presence of Fe^{3+} and mixed Fe^{3+} and Fe^{2+} oxyhydroxides is due to dissolved oxygen in the groundwater (*19*). Highly reduced conditions occurred throughout the barrier (mostly <−100 mV), except at the eastern up-gradient background water (TMW 12) (Figure 2a; Table 1). Most of the groundwater pH values were alkaline and were highest for DP 19M (7.2−10.4) near the western down-gradient end of the barrier (Figure 2b). Near neutral pH values were from the eastern up-gradient background well (TMW 12) (6.5−6.8) and the groundwater entering the eastern and northern up-gradient portion of the barrier at DP 22M (5.9−6.9). There is only a slight possibility that indigenous Fe oxides were present in the barrier due to low amounts of total Fe detected in the groundwater (*19*).

Akaganeite (β-FeOOH) was detected by XRD throughout the cores retrieved from the Fe^0 barrier. The poorly crystalline akaganeite is easily formed and stable under the reduced groundwater conditions of the Fe^0 barrier, which explains the widespread presence. The XRD and SEM-EDX analysis also revealed the presence of goethite (α-FeOOH) (Figures 3 and 4a) within the Fe^0 barrier, but it occurred to a lesser extent as compared to akaganeite. The lack of widespread distribution of this mineral throughout the barrier at the Y-12 site was perhaps due to the strongly reducing environment. Some oxidation of the barrier material had to occur for goethite to have formed. This may have been due to seasonal fluctuations of the groundwater table or due to the dissolved O_2 in groundwater. During these less reductive periods, the poorly crystalline akaganeite may have transformed into the more crystalline goethite (*23*). Geothite was the most abundant Fe oxyhydroxide phase present in the Fe^0 permeable barrier at the U.S. Coast Guard Center at Elizabeth City, NC which has been installed to remove Cr(IV) from the groundwater (*24*). The decrease of the Cr(IV) from the groundwater in this barrier is thought to be due to the reduction of Cr(IV) to Cr(III) which complexes with Fe(III) to form Fe(II) −Cr(II) oxyhydroxide phases as suggested by mineralogical studies of Fe^0 batch and column experiments (*3*). The groundwater at the U.S. Coast Guard Center site had a slight pH increase (>6.1) and a decrease in Eh (0−200 mV) in the barrier compared to untreated groundwater which had a pH of 5.6−5.9 and an Eh of >400 mV (*24*). These values suggest that there was less reducing conditions in the Elizabeth City Fe^0 barrier, compared to the Y-12 barrier, which explains the abundance of geothite and the absence of akaganeite. Lepidocrosite, which has been reported in laboratory Fe^{2+} column studies (*6*), was not detected in the Y-12 Fe^0 barrier material. The apparent absence of this mineral may be due to relatively high carbonate/bicarbonate contents of the groundwater at the study site. The presence of CO_2 was found to favor the formation of goethite over lepidocrosite in soils (*25*). Bicarbonate/carbonate ranged from 17 to 650 mg/L at the study site with the highest amount present in groundwater from the eastern up-gradient background water (TMW12) (330−650 mg/L) and at the entrance of the Fe^0 barrier at DP 22M (460−590 mg/L) (Figure 2c).

Calcium and Iron Carbonate Precipitates. Carbonate minerals, especially aragonite ($CaCO_3$), were present at the depths of 15−21′ of the Fe^0 barrier and in the deeper Section A core material from 22′−28′ (Figure 3) near where the groundwater entering the Fe^0 media from the northern and eastern up-gradients. Clusters of needle-shaped $CaCO_3$ crystals (Figure 4b) characteristic of aragonite were observed by SEM-EDX throughout the core material at these locations. This type of aragonite crystalline morphology has also been observed by SEM in samples from Fe^0 columns flushed with Ca^{2+} and CO_3^{2-} (*20, 26, 27*). In the 22−28′ deep Section A cores, aragonite decreased in frequency from the northern up-gradient to the southern down-gradient.

Groundwater at the study site contains both high Ca^{2+} and bicarbonate/carbonate because early operations at the site had leached calcareous Nolichucky shale bedrock with strong nitric acid. This was followed by neutralization of the acid by limestone in 1984 (*18*). The background Ca^{2+} concentration was around 200 mg/L in TMW 12 (Figure 2d),

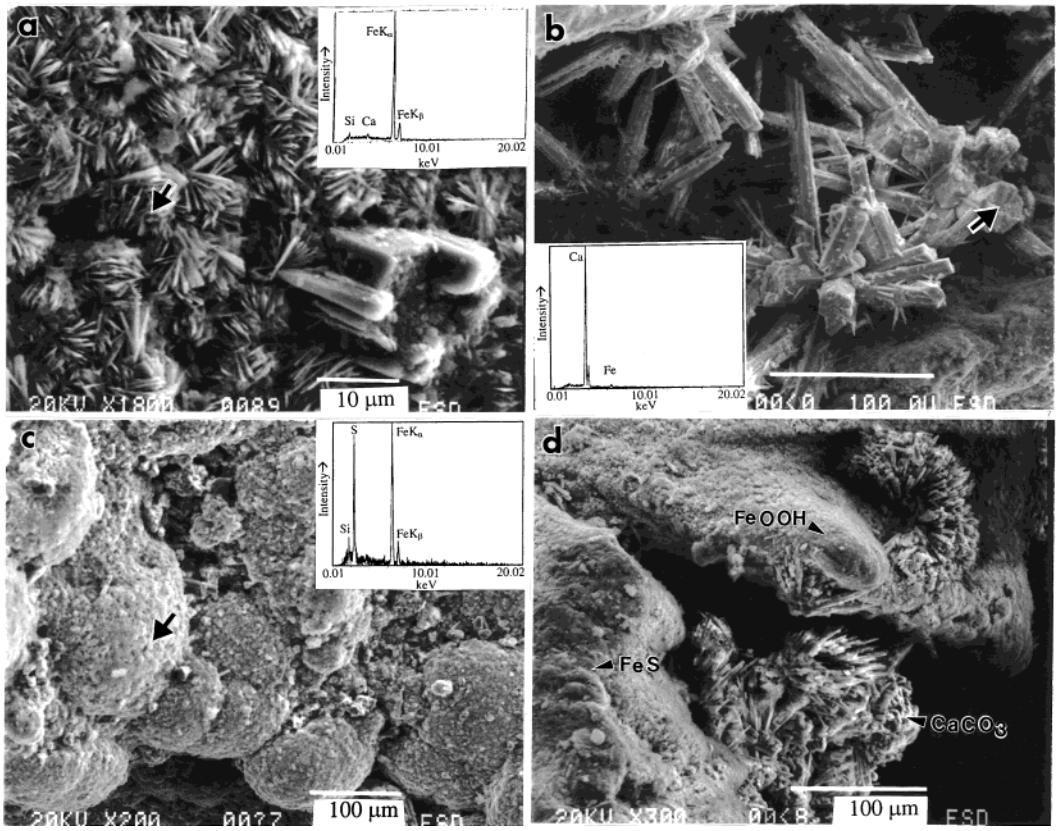

FIGURE 4. Mineral precipitates identified by SEM-EDX on the surfaces of Fe^0 filings in the barrier: (a) hexagonal shaped crystals of goethite (β-FeOOH) around an aragonite crystal (lower right corner) from the deep up-gradient Section A at the interface of the Fe^0 barrier and soil, (b) clusters of aragonite ($CaCO_3$) crystals in the mid-section of shallow up-gradient Section A, (c) rounded formations of amorphous FeS from the deep up-gradient Section A, and (d) precipitates of aragonite, amorphous FeS and FeOOH on the surfaces of an Fe^0 filing from the shallow down-gradient Section C at the interface of the soil and barrier.

where the concentration of Ca^{2+} in Fe^0 medium (DP 19 and DP22) varied considerably. In well DP 22, Ca^{2+} concentration was lower in the groundwater at the 18′ depth than at the 26′ depth according to samples from DP 22S and DP22M, respectively (Figure 2d). The occurrence of $CaCO_3$ precipitates and the lowering of Ca^{2+} in water samples at 15−21′ are attributed to an increased groundwater pH, which favored the formation or precipitation of $CaCO_3$ (Figure 2c,d). Similar findings have been reported for the Denver Federal Center Fe^0 reactive barrier, which was installed to mediate chlorinated aliphatic hydrocarbons. In this barrier, increased groundwater pH (9.7) in the gate compared to a pH of 7.1 outside the gate is also thought to be responsible for carbonate mineral precipitation, particularly $CaCO_3$, and the consequent decreased concentration of Ca^{2+} (*15*). Precipitation of aragonite in the 22−28′ zone at the entrance of the barrier (Section A) is less extensive because of a relatively low pH (5.9−6.9), thus depleting Ca^{2+} to a lesser degree. Compared to that in the 22−28′ eastern up-gradient well (DP 22M), the Ca^{2+} content was much lower in the 22−28′ western down-gradient well (DP 19M). The depletion of Ca^{2+} in the groundwater is from aragonite precipitation in the upper zone. This lowering of the Ca^{2+} concentration explains why there was no aragonite in the cores at depths of 22−28′ from Sections B and C.

Siderite ($FeCO_3$) was only detected in the Fe^0 samples by XRD at 15′ near and at the interface of the Fe^0 filings and soil at the northern up-gradient portion of Section A where groundwater enters the barrier (Figures 1a and 3). Several factors may contribute to the above observations. A relatively high pH and high carbonate but low calcium concentrations favor the formation of siderite. On the other hand, a relatively low pH (about neutral) and a low carbonate concentration shift the chemical equilibrium in favor of $Fe(OH)_2$ precipitation. High calcium concentrations in groundwater also compete with the ferrous iron for carbonate and form $CaCO_3$, as discussed previously. Similarly siderite precipitation has been observed throughout (*27*) and at the influent end (*25*) of Fe^0 columns treated with solutions containing Ca^{2+} and CO_3^-. These conditions are observed at DP22S near where siderite was present.

Iron Sulfide (FeS) Precipitate. Iron sulfide (FeS) was detected by SEM-EDX across the 15−21′ in the Fe^0 media and at the depths of 22′ in the northern up-gradient cemented areas in Section A at the interface of soil and Fe^0 barrier (Figure 3). Three-dimensional observations of FeS by SEM-EDX revealed this mineral as bytrodial shaped formations occurring as coatings and as part of the cemented material (Figure 4c). Visually, this type of formation appeared similar to spherical shaped framboids as described by van Dam and Pons (*29*) and Doner and Lynn (*28*) that contain pyrite microcrystallites. However, SEM-EDX analysis of polished sections showed that the FeS formations in the Fe^0 barrier occurred as coatings on the Fe^0 filings and mineral precipitates surrounding Fe^0 filings. The rounded morphology of FeS comes from the underlying material, particularly the rounded clusters of aragonite crystals, although FeS could also be produced as rounded formations as a result of microbiological activity (*19*). The FeS present in the barrier may not have been detected by XRD because of either noncrystallinity of the FeS structure or too small of an amount for detection. However, amorphous FeS is commonly observed in the samples by SEM and EDX analysis (*6*); therefore, lack of detection is perhaps due to noncrystallinity. This noncrystalline FeS is generally the first phase of FeS to precipitate; however, it may eventually undergo crystallation

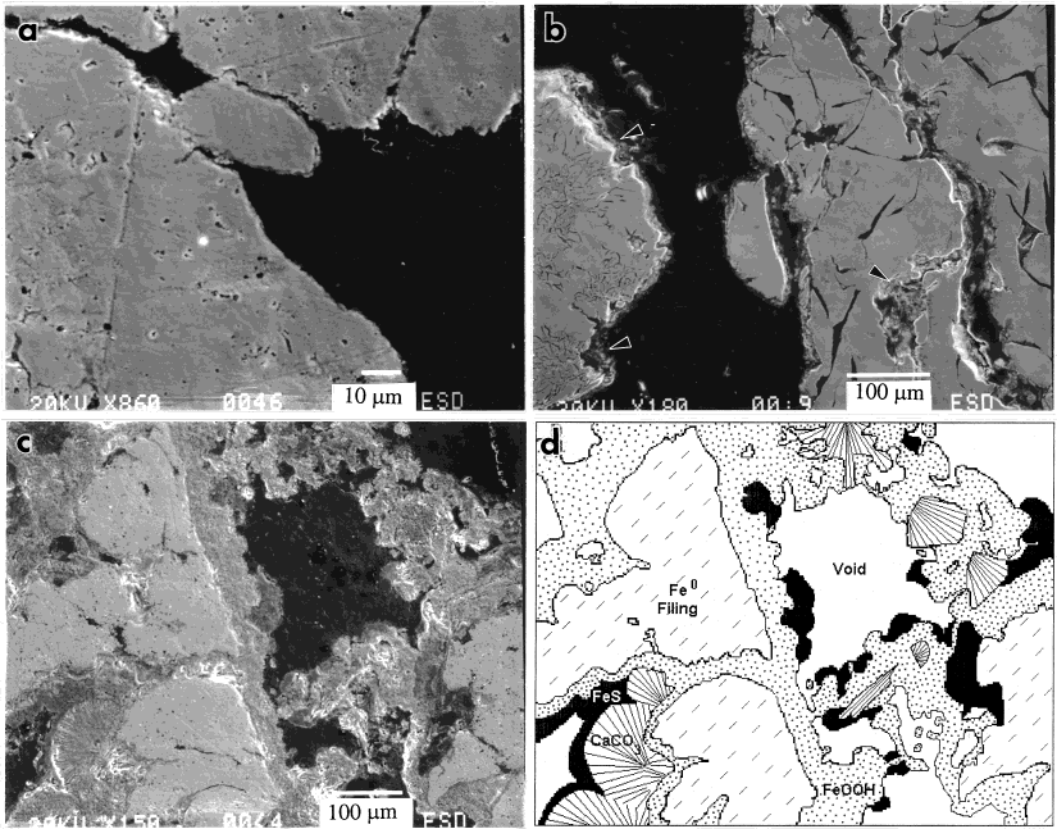

FIGURE 5. Polished cross-sections of Fe^0 filings showing corrosion and cementation in the Fe^0 barrier: (a) fresh Fe^0 filing showing trace amounts of corrosion (FeOOH) on the surface, (b) thin weathering rind on an Fe^0 filing from the shallow zone of Section B in the middle of the barrier, (c) cementation from the deep zone of Section A, and (d) outline of (c) showing Fe^0 filings bound together by FeOOH, aragonite and coated with amorphous FeS.

(*28*). Other studies also report FeS precipitation in reactive barrier material (*6*, *20*, *30*). Amorphous FeS (*7*) and the poorly crystalline mackinawite (tetragonal structure) (*20*) has been observed at the ×625 groundwater treatment facility, Portsmouth, OH. In addition, mackinawite has also been identified in a permeable reactive barrier containing a mixture of compost (20%), leaf mulch (20%), wood chips (9%), gravel (50%), and limestone (1%) used to treat metals and acid mine drainage (*30*).

There was a larger amount of FeS in the 15−21′ zone as compared to the 22−28′ zone of the barrier, probably induced by the presence of sulfate reducing microbes within the iron barrier (*19*). The guar gum that was used during the construction of the barrier may have stimulated the growth of the sulfate reducing bacteria and therefore the reduction of sulfate to sulfide. Analysis of microbial activity using phospholipid fatty acids (PLFA) techniques indicated that sulfate reducing bacteria were present in the iron zone (*19*). Microbial activity in the iron was consistently greater in the cores from 15 to 21′ zone than that from the 22−28′ zone. The concentration of sulfate in background wells was generally over 80 mg/L. However, in many of the 18′ and 26′ level piezometers within the iron, the concentration of sulfate was consistently less than the 1 mg/L, suggesting sulfate was being reduced microbially at these locations (*16*). An odor was also detected during groundwater sampling of the well from this section. Sulfate concentrations from piezometers at 31′ below the surface of the iron averaged over 40 mg/L in April 1999 (*19*), suggesting that sulfate reduction was not as prevalent in the 31′ section of the iron as it was in the 18′ zones. High concentrations of nitrate, often greater than 100 mg/L (*19*) in the 26 and 31′ sections of the iron (compared to <1 mg/L in the 18′ zone), may favor microbial reduction of nitrate rather than sulfate reduction (*31*) in the 26 and 31′ zones. The lower microbial activity and high nitrate concentration which favor nitrate reducing bacteria over sulfate reducing bacteria in the deeper sections of the iron were probably the primary reasons FeS precipitates were only observed in the 15−21′ zone of the iron.

Corrosion Rate and Cementation of Iron. Mostly thin and discontinuous, corrosion rinds were observed on individual Fe^0 filings from Sections A and C, while only a trace of corrosion was present on filings from Section B as compared to fresh Fe^0 filings (Figure 5a,b). The rinds generally ranged in thickness from 2 to 20 μm in Sections A and C. However, thicker rinds were observed on some of the individual Fe^0 filings (10−50 μm) and on Fe^0 filings from the cemented areas (10−150 μm) at Section A. Much of the surfaces of the Fe^0 filings are still not corroded, except in the northern up-gradient Sections A and southern down-gradient Section C. According to SEM examinations, these rinds are not pseudomorphic replacements but instead are the weathered portion of the Fe^0 filings. Although there is a possibility that the rinds could be Fe hydroxide deposits, the morphology of the rinds on these Fe^0 filings appear as disintegrated portions of the filings. Deposits of other minerals such as carbonates and FeS which are readily detected by SEM-EDX and do not appear to be a source of these weathering rinds. Based on the worst corrosion (150 μm) that had occurred in the 15 months of operation (at a rate of 10 μm/mm) as observed by SEM, it appeared that these filings would last longer than 15 years for Fe^0 filings from the midsection of the barrier. However, it is pointed out that this number (15 years) should be regarded as a rough estimate at the best because it is solely based on the visual inspection of the corrosion rinds of the polished section samples. The thickness of the corrosion rinds or the rate of iron corrosion will depend largely on the geochemistry of groundwater. For example,

Agrawal and Tratnyek (*32*) report that corrosion of Fe^0 can be increased by the reduction of H_2CO_3 and HCO_3^-. Similar rinds, described as oxyhydroxide layers of 10−20 μm, were also observed on Fe^0 filings in a column study where HCO_3^- and SO_4^{2-} was flushed through the system (*6*).

Comparisons of polished sections of individual Fe^0 filings throughout the barrier and cemented samples from Section A by SEM-EDX revealed that more corrosion occurred in the cemented samples as compared to the loose individual Fe^0 filings (Figure 5a−c). In the cemented samples, corrosion appeared as thick rinds of Fe oxyhydroxides, FeOOH, sometimes binding individual filings together. Signs of degeneration, such as cracking and breaking apart, occurred on some of the Fe^0 filings beneath the rind. These features do not appear to be artifacts created from sample preparation. These rinds ranged in thickness from ∼10 to ∼150 μm. With the average Fe^0 filing being 3 to 23 mm long (majority ≥10 mm) and 0.5 to 1.25 mm thick, the corrosion appeared to have degenerated approximately 15−30% of the Fe^0 filings in the cemented samples. According to visual estimates, if corrosion continues, these Fe^0 filings will be completely corroded in 5 to 10 years under the specific Y-12 geochemical conditions. However, cemented filings were a small portion of the total Fe^0 from the cores collected from the barrier. Because of precipitates of Fe oxyhydroxides, aragonite, and FeS which form coatings on Fe^0 filing surfaces, there is uncertainty as to if the degeneration will continue in these units (Figure 4d). The accumulation of some precipitates, such as $CaCO_3$ and $FeCO_3$, may eventually prevent corrosion by limiting mass transfer to the metal surface. The consequence is the surface reactivity of the Fe^0 filings will decrease.

Cementation of Fe^0 filings was observed from the depths of 18−22′ in Section A where groundwater first enters the Fe^0 portion of the barrier (Figure 3). It appeared from our study and others (*11, 15*) that cementation due to the precipitation of FeOOH, $CaCO_3$, and $FeCO_3$, either individually or in combination, generally occurs at the interface where groundwater first enters the Fe^0 system. Based on SEM-EDX analysis and observations of polished sections, the cementation in the Y-12 barrier appeared to be mainly a result of an accumulation of FeOOH. Mackenzie et al. (*10*) described the portion of an Fe^0 column clogged with FeOOH as hardened solid masses that greatly decreased hydraulic permeability. Additionally, smaller amounts of crystalline aragonite acted at least partially as a binding agent (Figure 5c,d) in the cemented areas in the Y-12 barrier. Calcium carbonate precipitation has also resulted in cementation in an Fe^0 barrier (*15*) and in an ex situ reactor as a binding agent along with $FeCO_3$ and FeOOH (*11*). However, $CaCO_3$ was found to have played no role in the clogging of an Fe^0 column which was cemented by FeOOH as reported by MacKenzie et al. (*5*). SEM-EDX analysis polished sections from the Y-12 barrier revealed FeS existing primarily as a binding agent in the form of coatings and void fillers (Figure 5c,d). Additionally, more precipitates (fine materials) of FeS were observed at a depth of 18−21′ from the northern up-gradient to the southern down-gradient in Section A compared to the other cores.

The sequence of surface precipitation on Fe^0 filings as observed by SEM of the polished sections appeared to be in agreement with the geochemical data. Iron oxyhydroxides precipitated first as a corrosion byproduct of the Fe^0 in oxygenated groundwater. Not only were the Fe oxyhydroxides observed as corrosion rinds on the Fe^0 filings, but also they bound individual filings together. The formation of aragonite followed in response to an increase in CO_3^- in the alkaline-pH waters, which is a direct result of iron corrosion. Iron sulfide was found in cores recovered near groundwater sampling points, where SO_4^{2-} was reduced to S^-. The delay in formation of FeS compared to the other precipitates in the trench was perhaps due to the greater length of time needed for an accumulation of a microbial population to facilitate SO_4^{2-} reduction.

Continual formation of mineral precipitates would eventually reduce the groundwater flow rate and alter the flow pattern through the barrier; thus, reducing the long-term performance of this Fe^0 barrier to remove uranium and other contaminants. Cementation in the 22′ northern up-gradient of Section A was denser as compared to the 18−21′ down-gradient cementation of Section A. This may be due to a greater amount of Fe oxyhydroxides and aragonite as binding material. McMahon et al. (*14*) calculated a 0.35% yearly loss of total porosity in the reactive media for the Denver Federal Center site where there was an accumulation of $CaCO_3$. This would not be a substantial loss if the mineral precipitates were uniformly distributed throughout the barrier gate. However, dissolved inorganic carbon and Ca^{2+} data indicated that carbonate precipitated in the up-gradient interface (gate) to the barrier. Such an uneven distribution of precipitates would result in an early change of hydraulic conductivity, thus affecting the flow through the barrier. This is of great concern to the long-term performance of permeable Fe^0 reactive barriers. Therefore, close attention should be given to areas in barriers that seem more vulnerable to corrosion (i.e. where groundwater first enters barriers), precipitation, and subsequent cementation of Fe^0 filings.

From the hydrology data at the site, the cementation does not appear to be affecting the movement of groundwater through the barrier; therefore, it is probably isolated in a small area at the up-gradient portion of the Fe^0 filings. Note that the areas of cementation were observed in the 1 1/4″ diameter cores collected at Section A. In the 18−21′ section of Section A, loose Fe^0 filings and small clumps of Fe^0 filings that were cemented together surrounded larger zones of cemented filings. In the Section A core, cementation decreased from 70% at the southern down-gradient interface (12.5 cm length section of the core) to 40% in the middle of this coring section (12.5−25 cm from the down-gradient interface). Additionally, at the 22′ northern up-gradient soil and Fe^0 filing interface (12.5 cm length section of the core) of Section A, 30% of the interface Fe^0 filings was cemented. The hydraulic gradient between TMW11 located in the barrier just up-gradient of the Fe^0 section and TMW7 located in the trench just down-gradient of the Fe^0 section is consistently from east to west down the trench with an average gradient of 0.007 across the entire iron section over a 15 month period. If substantial cementation of the iron had occurred during the past 15 months, the gradient across the iron would likely increase over time to compensate for the decrease in hydraulic conductivity of the iron. However, the increases and decreases in gradient observed over the past 15 months appear to be related to seasonal fluctuations in groundwater elevations not to any long-term increasing trends related to cementation. As might be expected, gradients are generally higher when groundwater levels are higher and groundwater flow is greatest. Continuous groundwater level measurements with data loggers and transducers show that the east to west gradient down the trench is maintained during large rainfall recharge events (*19*).

Acknowledgments

The authors thank M. K. McCracken for assistance with the collection of cores and Charles M. McNulty, Mary Anna Bogle, Norman D. Farrow, M. Dickey, and D. A. Abbot for their help with groundwater sampling and collecting field parameters. We also thank four anonymous reviewers for their constructive comments on the manuscript. Core samples were collected compliments of MSE Inc. Funding for this research was supported by the subsurface Contaminants Focus Area, Office of Environmental Management (EM) of the U.S. Department of Energy (DOE). Oak Ridge National Laboratory

(ORNL) is managed by University of Tennessee-Battelle LLC under contract DE-AC05-00OR22725. D. H. Phillips and Y. Roh are supported by the postdoctoral fellowship program administrated by Oak Ridge Institute for Science and Education. Environmental Sciences Division Publication No. 5033.

Literature Cited

(1) Gillham, R. W.; O'Hannesin, S. F. Metal-catalysed abiotic degradation of halogenated organic compounds; Presented at the IAH Conference Modern Trends in Hydrogeology; Hamilton, Ontario, Canada, 1992; pp 94−103.
(2) Matheson, L. J.; Tratnyek, P. G. *Environ. Sci. Technol.* **1994**, *28*, 2045−2053.
(3) Blowes, D. W.; Ptacek, C. J.; Jambor, J. L. *Environ. Sci. Technol.* **1999**, *31*, 3348−3357.
(4) Qui, S. R.; Lai, H,-F.; Robertson, M. J.; Hunt, M. L.; Amrheim, C.; Giancarlo, L. C.; Flynn, G. W.; Yarmoff, J. A. *Langmuir* **2000**, *16*, 2230−2236.
(5) Gu, B.; Liang, L.; Dickey, M. J.; Yin, X.; Dai. S. *Environ. Sci. Technol.* **1998**, *32*, 3366−3373.
(6) Gu, B.; Phelps, T. J.; Liang, L.; Dickey, M. J.; Roh, Y.; Kinsall, B. L.; Palumbo, A. V.; Jacobs, G. K. *Environ. Sci. Technol.* **1999**, *33*, 2170−2177.
(7) Roh, Y.; Lee, S. Y.; Elless, M. P.; Moon, H.-S. *J. Environ. Sci. Health*. **2000**, *35* (in press).
(8) Roh, Y.; Lee, S. Y.; Elless, M. P.; Cho, K.-S. *J. Environ. Sci. Health*. **2000**, *35* (in press).
(9) RTFD web site: WWW.RTFD.ORG.
(10) Mackenzie, P. D.; Sivavec, T. M.; Horney, D. P. *International Containment Technology Conference and Exhibition*; St. Petersburg, FL, 1997; pp 781−786.
(11) Shoemaker, S. H.; Greiner, J. F.; Gillham, R. W. In *Assessment of Barrier Containment Technologies*; Rumer, R. R., Michell, J. K., Eds.; U.S. Department of Energy; Washington, DC, 1995; pp 301−353.
(12) Liang, L.; Korte, N.; Gu, B.; Puls, R.; Reeter, C. *Adv. Environ. Res.* **2000**, (in press).
(13) Blowes, D. W.; Ptacek, C. J.; Cherry, J. A.; Gillham, R. W.; Robertson, W. D. Geotechnical Special Publication No. 46; Acar, Y. B., Daniel, D. E., Eds.; American Society of Civil Engineers: New York, 1995; Vol. 2, pp 1588−1607.
(14) McMahon, P. B.; Dennehy, K. F.; Sandstrom, M. W. *Ground Water* **1999**, *37*, 396−405.
(15) Odziemkowskie, M.; Schumacher, T. T.; Reardon, E. J. *Corros. Sci.* **1998**. *40*, 371−389.
(16) Liang, L.; West, O. R.; Korte, N. E.; Goodlaxson, J. D.; Pickering, D. A.; Zutman, J. L.; Anderson, F. J.; Welch, C. A.; Pelfrey, M. J.; Dickey, M. J. *A field-scale test of trichloroethylene dechlorination using iron filings for the X-120/X-749 groundwater plume*; ORNL/TM-13217; Oak Ridge National Laboratory: Oak Ridge, TN, 1997.
(17) Edwards, R. W.; Duster, D.; Faile, M.; Gallant, W.; Gilbeau, E.; Myller, B.; Nevling, K.; O'Brady, B. Presented at RTDF Permeable Reactive Barriers Action Team Meeting; San Francisco, CA, August 15−16, 1996.
(18) Watson, D.; Leavett, M,; Smith, C.; Klasson, T.; Bostick, B.; Liang, L.; Moss, D. *Bear Creek Valley Characterization Area Mixed Wastes Passive In Situ Treatment Technology Demonstration Project- Status Report*; Presented at the International Containment Technology Conference and Exhibition, St. Petersburg, FL, 1997; pp 730−736.
(19) Watson, D.; Gu, B.; Phillips, D. H.; Lee, S. Y. *Evaluation of Permeable Reactive Barriers for Removal of Uranium and other Inorganics at the Department of Energy Y-12 Plant, S-3 Disposal Ponds*; ORNL/TM-1999-143; Oak Ridge National Laboratory: Oak Ridge, TN, 1999.
(20) Roh, Y.; Lee, S. Y.; Elless, M. P. *Enivron. Geol.* (in press) **2000**.
(21) Gu, B.; Melhorn, T. l.; Liang, L.; McCarthy, J. F. *Geochim. Cosmochim. Acta* **1996**, *60*, 2977−2992.
(22) McKee, T. R.; Brown, J. L. In *Minerals in Soil Environments*; Dixon, J. B., Weed, S. B., Eds.; Soil Science Society of America: 1977; pp 809−846.
(23) Schwertmann, U.; Cornell, R. M. *Iron Oxides in the Laboratory: Preparation and Characterization;* VCH Publishers: New York, 1991*;* 137p.
(24) Blowes, D. W.; Puls, R. W.; Bennett, T. A.; Gillham, R. W.; Hanton-Fong, C. J.; Ptacek, C. J. *International Containment Technology Conference and Exhibition*; St. Petersburg, FL, 1997; pp 851−857.
(25) Schwertmann, U.; Taylor, R. M. In *Minerals in Soil Environments*; Dixon, J. B., Weed, S. B., Eds.; Soil Science Society of America: 1977; pp 145−180.
(26) Schuhmacher, T.; Odziemkowski, M. S.; Reardon, E. J.; Gillham, R. W. *Identification of Precipitates Formed on Zerovalent Iron in Anaerobic Aqueous Solutions*; Presented at the International Containment Technology Conference and Exhibition; St. Petersburg, FL, 1997; pp 801−805.
(27) Mackenzie, P. D.; Horney, D. P.; Sivavec, T. M. *J. Haz. Materials* **1999**, *68*, 1−17.
(28) Doner, H. E.; Lynn, W. C. In *Minerals in Soil Environments*; Dixon, J. B., Weed, S. B., Eds.; Soil Science Society of America: 1977; pp 75−98.
(29) van Dam, D.; Pons, L. J. In *Acid Sulphate Soils*; ILRI Publication 18; Dost, H., Eds.; International Institute for Land Reclamation and Improvement: Wageningen, 1973; Vol. II, pp 169−196.
(30) Benner, S. G.; Blowes, D. W.; Gould, W. D.; Herbert, R. B., Jr.; Ptacek, C. J. *Environ. Sci. Technol.* **1999**, *33*, 2793−2799.
(31) Weidemeir, T.; Wilson, J. T.; Kampbell, D. H.; Miller, R. N.; Hansen, J. E. *Technical Protocol for Implementing Intrinsic Remediation with Long-Term Monitoring for Natural Attenuation of Fuel Contamination Dissolved in Groundwater*; Air Force Cent. of Environ. Excell., Technol. Trans. Div, Brooks AFT: San Antonio, 1995.
(32) Agrawal, A.; Tratnyek, P. G. *Environ. Sci. Technol.* **1996**, *30*, 153−160.

Received for review February 14, 2000. Revised manuscript received June 29, 2032. Accepted July 19, 2000.

ES001005Z